Synthesis and Structure of Two New Ternary Nitrides: $FeWN_2$ and $MnMoN_2$

David S. Bem, Christina M. Lampe-Önnerud, Hans P. Olsen, and Hans-Conrad zur Loye*

Department of Chemistry, Massachusetts Institute of Technology, Cambridge, Massachusetts 02139

Received September 25, 1995[⊗]

New layered ternary transition metal nitrides, $FeWN_2$ and $MnMoN_2$, were synthesized in single-step reactions by the ammonolysis of ternary transition metal oxides. Solid-state precursors $FeWO_4$ and $MnMoO_4$ were treated with ammonia at 625 and 800 °C to yield the ternary nitrides $FeWN_2$ ($P6_3/mmc$; a = 2.87630(5) Å, c = 10.9320(4) Å) and $MnMoN_2$ ($P6_3/mmc$; a = 2.92262(8) Å, b = 10.8564(4) Å), respectively. Structures are proposed on the basis of Rietveld analysis of powder X-ray diffraction data. These compounds are members of a family of layered hexagonal ternary nitrides, consisting of alternating layers of MN_6 (M = Fe, Mn) octahedra and $M'N_6$ (M′ = W, Mo) trigonal prisms. The conductivity data for both compounds indicate metallic-like behavior.

Introduction

Solid state nitrides have received increased attention in recent years, and several research groups are pursuing their syntheses and characterization.[1−11] In general, nitrides have lower decomposition temperatures than oxides, due to the high bond energy of N_2 (941 kJ/mol) compared to O_2 (499 kJ/mol).[12] Consequently, high-temperature techniques have provided only limited success in the preparation of ternary nitrides and low- to moderate-temperature approaches become essential for preparing both metastable (kinetic) and stable (thermodynamic) compounds. One successful approach has been the use of molecular precursors to make thin films and powders of binary nitrides.[13−15] Ternary nitrides have been synthesized by reacting a transition metal or main group element with an alkali or alkaline earth nitride/amide, yielding numerous new phases,[2,3,8,10,11,16−22] including Ca_6FeN_5,[19] Li_3FeN_2,[23] or $NaTaN_2$.[24] Another approach for synthesizing alkali-metal-containing ternary nitrides has been the use of ternary oxide precursors; for example, the ternary nitride $LiMoN_2$ can be synthesized by reaction between Li_2MoO_4 and NH_3(g).[5]

Although these synthetic methods have been successful, almost all take advantage of the inductive effect, which stabilizes the M−N bond by donation of electrons from an electropositive element.[12,25] This approach limits the number of potential new ternary nitrides to those containing a highly electropositive element such as an alkali or alkaline earth metal. In the absence of inductive effect stabilization, the formation of binary nitrides rather than ternary nitrides is favored at the high temperatures necessary for reactions (>1000 °C).[26,27] Our approach, the ammonolysis of ternary oxides,[5,26,28−32] has been shown to be a successful low-temperature route in nitride synthesis. The use of ternary oxide precursors offers the advantage of atomic-level mixing of the metals, which decreases the diffusion distances of the cations and which may lower the temperature necessary for reaction. In this paper we report on two new ternary nitrides, $FeWN_2$ and $MnMoN_2$, synthesized from ternary oxide precursors.

Experimental Section

Precursor Synthesis. (a) $FeWO_4$. Iron tungstate, $FeWO_4$, was prepared by dropwise addition of 40 mL (0.25 M) of an aqueous solution of iron chloride, $FeCl_2$ (Cerac, 99.99%, weighed in Ar

* To whom correspondence should be addressed.

[⊗] Abstract published in *Advance ACS Abstracts,* January 1, 1996.

(1) Chern, M. Y.; DiSalvo, F. J.; Parise, J. B.; Goldstone, J. A. *J. Solid State Chem.* **1992**, *96*, 426−435.
(2) Chern, M. Y.; DiSalvo, F. J. *J. Solid State Chem.* **1990**, *88*, 528−533.
(3) Chern, M. Y.; DiSalvo, F. J. *J. Solid State Chem.* **1990**, *88*, 459−464.
(4) Gudat, A.; Haag, S.; Kniep, R.; Rabenau, A. *J. Less-Common Met.* **1990**, *159*, L29−L31.
(5) Elder, S. H.; Doerrer, L. H.; DiSalvo, F. J. *Chem. Mater.* **1992**, *4*, 928−937.
(6) Jacobs, H.; Niewa, R. *Eur. J. Solid State Inorg. Chem.* **1994**, *31*, 105−113.
(7) Jacobs, H.; von Pinkowski, E. *J. Less-Common Met.* **1989**, *146*, 147−160.
(8) Rauch, P. E.; DiSalvo, F. J. *J. Solid State Chem.* **1992**, *100*, 160−165.
(9) Rauch, P. E.; DiSalvo, F. J.; Brese, N. E.; Partin, D. E.; O'Keeffe, M. *J. Solid State Chem.* **1994**, *110*, 162−166.
(10) Vennos, D. A.; Badding, M. E.; DiSalvo, F. J. *Inorg. Chem.* **1990**, *29*, 4059−4062.
(11) Vennos, D. A.; DiSalvo, F. J. *J. Solid State Chem.* **1991**, *98*, 318−322.
(12) DiSalvo, F. J. *Science* **1990**, *247*, 649−655.
(13) LaDuca, R. L.; Wolczanski, P. T. *Inorg. Chem.* **1992**, *31*, 1311−1313.
(14) Winter, C. H.; Sheridan, P. H.; Lewkebandara, T. S.; Heeg, M. J.; Proscia, J. W. *J. Am. Chem. Soc.* **1992**, *114*, 1095−1097.
(15) Holl, M. M. B.; Wolczanski, P. T.; Van Duyne, G. D. *J. Am. Chem. Soc.* **1990**, *112*, 7989−7994.
(16) Brokamp, T.; Jacobs, H. *J. Alloys Compd.* **1991**, *176*, 47−60.
(17) Cordier, G.; Gudat, A.; Kniep, R.; Rabenau, A. *Angew. Chem.* **1989**, *101*, 1689−1690.
(18) Cordier, G.; Gudat, A.; Kniep, R.; Rabenau, A. *Angew. Chem.* **1989**, *101*, 204.
(19) Cordier, G.; Höhn, P.; Kniep, R.; Rabenau, A. *Z. Anorg. Allg. Chem.* **1990**, *591*, 58−66.
(20) Chern, M. Y.; Vennos, D. A.; DiSalvo, F. J. *J. Solid State Chem.* **1992**, *96*, 415−425.
(21) Juza, R.; Langer, K.; Von Benda, K. *Angew. Chem.* **1968**, *80*, 373−384.
(22) Gudat, A.; Milius, W.; Haag, S.; Kniep, R.; Rabenau, A. *J. Less-Common Met.* **1991**, *168*, 305−312.
(23) Gudat, A.; Kniep, R.; Rabenau, A.; Bronger, W.; Ruschewitz, U. *J. Less-Common Met.* **1990**, *161*, 31−36.
(24) Zachwieja, U.; Jacobs, H. *Eur. J. Solid State Inorg. Chem.* **1991**, *28*, 1055−1062.
(25) Etourneau, J.; Portier, J.; Ménil, F. *J. Alloys Compd.* **1992**, *188*, 1−7.
(26) Marchand, R.; Laurent, Y.; Guyader, J.; L'Haridon, P.; Verdier, P. *J. Eur. Ceram. Soc.* **1991**, *8*, 197−213.
(27) Toth, L. E. *Transition Metal Carbides and Nitrides*; Academic Press: New York, 1971.
(28) Bem, D. S.; Houmes, J. D.; zur Loye, H.-C. In *MRS Symposium Proceeding*; Covalent Ceramics II: Non-Oxides; Barron, A. R., Fischman, G. S., Fury, M. A., Hepp, A. F., Eds.; Boston, MA, 1993; Vol. 327, p 150.
(29) Bem, D. S.; zur Loye, H.-C. *J. Solid State Chem.* **1993**, *104*, 467.
(30) Bem, D. S.; Gibson, C. P.; zur Loye, H.-C. *Chem. Mater.* **1993**, *5*, 397−399.
(31) Houmes, J. D.; Bem, D. S.; zur Loye, H.-C. In *MRS Symposium Proceeding*; Covalent Ceramics II: Non-Oxides; Barron, A. R., Fischman, G. S., Fury, M. A., Hepp, A. F., Eds.; Boston, MA, 1993; Vol. 327, p 153.
(32) Jaggers, C. H.; James, N. M.; Stacy, A. M. *Chem. Mater.* **1990**, *2*, 150−157.

0020-1669/96/1335-0581$12.00/0

glovebox) to a 15 mL (0.67 M) solution of sodium tungstate, $Na_2WO_4 \cdot 2\ H_2O$ (Aldrich, 99%). A brown precipitate was immediately observed, and the suspension was stirred for 1 h. A brown solid product was isolated by vacuum filtration and rinsed with two ~20 mL washings of water followed by a single ~20 mL washing with anhydrous ethanol. The solid was dried at 150 °C for 24 h and was amorphous by powder X-ray diffraction. Heating the amorphous precursor to 700 °C under He results in crystalline $FeWO_4$ (JCPDS 21-436).[33]

Crystalline iron tungstate, $FeWO_4$, was also prepared by solid state reaction. In a glovebox stoichiometric amounts of Fe (Aldrich, 99.99%), Fe_2O_3 (Cerac, 99.99%, −325 mesh), and WO_3 (Aesar, 99.8%) were ground together using an agate mortar and pestle. The powder was sealed in an evacuated quartz tube and heated at 5 °C/min to 900 °C, held at that temperature for 48 h, and then cooled at 10 °C/min to room temperature.

(b) $MnMoO_4$. Hydrated manganese molybdate, $MnMoO_4 \cdot 0.9\ H_2O$, was prepared by dropwise addition of 150 mL (0.363 M) of an aqueous solution of sodium molybdate dihydrate, $Na_2MoO_4 \cdot 2\ H_2O$ (Aldrich 99%) to a 200 mL (0.27 M) solution of manganese chloride, $MnCl_2$ (Cerac, 99.5%, weighed in Ar glovebox). A light yellow-green precipitate was immediately observed and the solution was stirred for 1 h. A yellow solid product was isolated by vacuum filtration and rinsed with two ~20 mL washings of water followed by a single ~20 mL washing with anhydrous ethanol. The solid was dried at 150 °C for 24 h. The product was identified as $MnMoO_4 \cdot 0.9H_2O$[34] by powder X-ray diffraction. Note that while other manganese molybdenum hydrates with different structures exist, only $MnMoO_4 \cdot 0.9H_2O$ leads to the ternary nitride product, $MnMoN_2$, when using the synthesis route described below.

Nitride Synthesis. $FeWN_2$ was synthesized by heating ~0.5 g of the oxide precursor, $FeWO_4$, under flowing ammonia. $FeWO_4$ was placed into an alumina boat, which was then inserted into a quartz flow-through reactor. The sample was heated at 5 °C/min to 700 °C and held at that temperature for 12 h under flowing ammonia gas (Airco, Anhydrous 99.99%; 150 cm^3/min). After 12 h, the sample was cooled rapidly by turning off the furnace and opening it to the air (cooled from 700 to 100 °C in ~20 min). The nitride product was removed from the system after cooling to room temperature.

$MnMoN_2$ was similarly synthesized by heating ~0.5 g of the oxide precursor, $MnMoO_4$, under flowing ammonia. $MnMoO_4$ was placed into an alumina boat, which was then inserted into a quartz flow-through reactor. The sample was heated at 5 °C/min to 625 °C and held at that temperature for 24 h under flowing ammonia gas (Airco, Anhydrous 99.99%; 150 cm^3/min). After 24 h, the sample was rapidly cooled by turning off the furnace and opening it to the air (cooled from 625 to 100 °C in ~18 min). Once the sample had cooled to room temperature, the nitride product was removed from the system. By trial and error, 700 and 625 °C were found to be the reaction temperatures that result in phase pure $FeWN_2$ and $MnMoN_2$, respectively. In either case, a pure product was only obtained over a narrow temperature range for a given flow rate. Attempts to dissolve these nitride products in acids or bases (HCl, HNO_3, aqua regia, H_2SO_4, HF, NaOH) were unsuccessful.

Characterization. (a) X-ray Diffraction. Powder X-ray diffraction patterns were collected using a Rigaku RU300 diffractometer operated with Cu Kα radiation. Qualitative phase analysis of the oxide precursors and the reaction products was performed using a continuous scan. Step-scanned diffraction patterns of $FeWN_2$ ($10° \le 2\theta \le 120°$, 0.03° steps) and $MnMoN_2$ ($10° \le 2\theta \le 140°$, 0.03° steps) were used for the Rietveld refinement. Rietveld refinements were performed using the General Structure Analysis System, GSAS.[35]

Elemental Analysis. The metal ratios and the oxygen content of the precursors and nitride products were determined on pressed pellets by energy-dispersive spectroscopy (EDS) on a JEOL JSM 6400 scanning electron microscope collected by a Noran Z-max windowless detector with quantification performed using virtual standards on associated Voyager software. The detection limit of the windowless EDS is 1 atom % for elements with an atomic number of 5 or higher. Nitrogen content was determined by C, H, N combustion analysis (Oneida). Thermogravimetric measurements (Cahn 121 TGA) were used to determine the water content of the precursors by heating the samples under He at 5 °C/min to 650 °C. The oxygen impurity content of $FeWN_2$ was also indirectly determined by heating the nitride sample to 900 °C under oxygen and comparing the observed weight increase with the C, H, N combustion analysis.

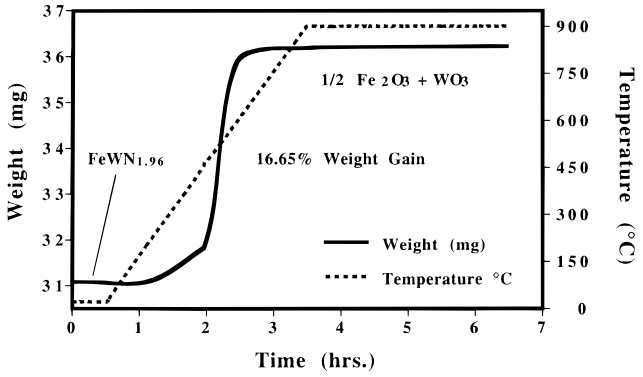

Figure 1. Thermogravimetric analysis of $FeWN_2$ heated under oxygen to 900 °C.

(c) Conductivity Measurements. Temperature-dependent four-probe resistivity measurements were performed on pressed pellets using a Keithley 236 Source Measure Unit and a Janis closed-cycle refrigerator (Model ccs-200) by measuring the voltage at a constant current of 50 mA. Pellets were pressed at 5000 psi in air. Attempts to sinter pellets by heating in a nitrogen atmosphere were unsuccessful due to sample decomposition.

Results

The metal content of the nitride products, as determined by energy-dispersive spectroscopy, agreed with that of the oxide precursor and was essentially 1:1 in both cases. (Fe:W ratio 49:51 (±3%) and Mn:Mo ratio 47:53 (±3%)). The nitrogen content of the nitride products as determined by C, H, N analysis was close to 2, $FeWN_2$ (1.97 ± 0.04) and $MnMoN_2$ (1.90 ± 0.04). The slight nitrogen deficiency has been observed in other related ternary nitrides, such as α- and β-$MnWN_2$ and $(Fe_{0.8}Mo_{0.2})MoN_2$.[31,36] The nitrogen content of $FeWN_2$ was also determined indirectly by thermogravimetric analysis. Figure 1 shows the mass change upon heating $FeWN_2$ in oxygen in a TGA apparatus, resulting in a brown powder which was identified by powder X-ray diffraction as a mixture of Fe_2O_3 and WO_3. The mass gain of 16.65 wt % is in agreement with the theoretical mass gain of 16.62 wt % for the oxidation of $FeWN_2$ to Fe_2O_3 and WO_3; the observed mass gain corresponds to an initial sample composition of $FeWN_{1.96}$, in good agreement with the results from C, H, N analysis. Thermogravimetric oxidation of $MnMoN_2$ was performed; however, the results were inconclusive due to the formation of several phases of manganese oxide. Oxygen analysis by windowless EDS did not detect any oxygen in the nitride samples, suggesting little or no oxygen uptake by the sample. Powder X-ray diffraction patterns of the samples exposed to the atmosphere for a period of 1 year did not change, confirming our observation that $FeWN_2$ and $MnMoN_2$ are stable to air and moisture.

Structure Refinements. (a) $FeWN_2$. It is possible to index the powder X-ray diffraction data of $FeWN_2$ with two hexagonal unit cells: $a = 2.867(2)$ Å, $c = 16.458(9)$ Å[29] and $a = 2.87630(5)$ Å, $c = 10.9320(4)$ Å presented here. On the basis of the systematic absences, the latter unit cell was chosen for

(33) Cid-Dresdner, H.; Escobar, C. *Z. Kristallogr.* **1970**, *127*, 61−72.
(34) Corbet, F.; Eyraud, C. *Bull. Soc. Chim. Fr.* **1961**, 571−574.
(35) Larson, A. C.; von Dreele, R. B.; Lansce. Report Los Alamos National Laboratory: MS-H805: Los Alamos, NM, 1993.
(36) Bem, D. S.; Olsen, H. P.; zur Loye, H.-C. *Chem. Mater.* **1995**, *7*, 1824.

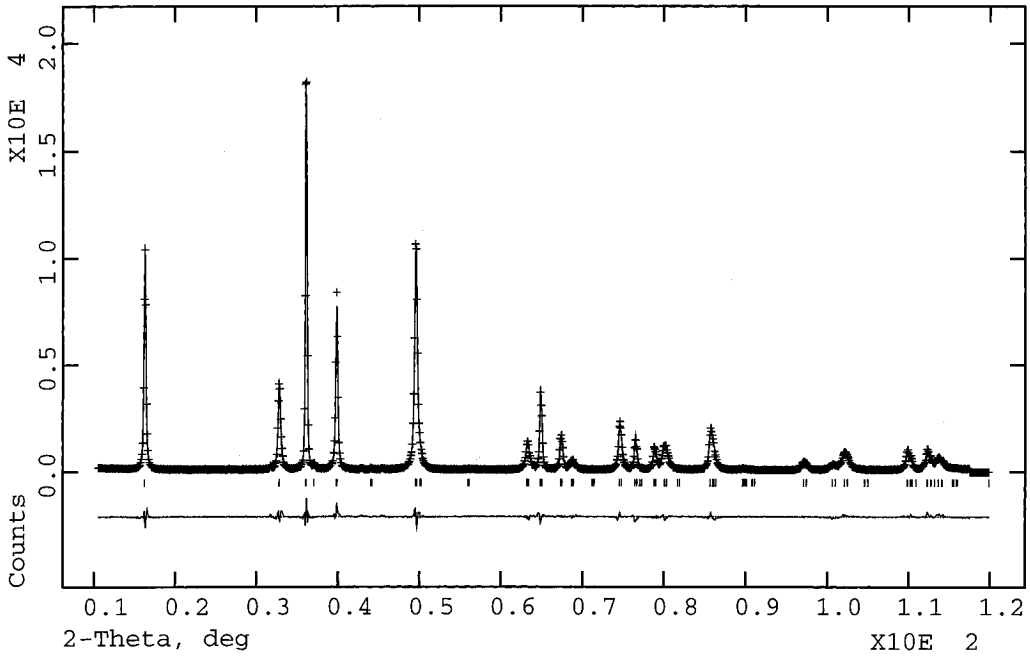

Figure 2. Observed (dotted) and calculated (solid line) X-ray profile for $FeWN_2$. Tic marks below the diffractogram represent allowed Bragg reflections. The difference line, observed minus calculated, is located at the bottom of the figure.

refinement in the space group $P6_3/mmc$ (No. 194), and on the basis of the metal coordination found in the layered ternary nitride $LiMoN_2$,[5] a structural model was constructed that consisted of hexagonally close-packed nitrogen sheets containing tungsten in trigonal prismatic and iron in octahedral coordination. The data were refined using the computer program GSAS.[35] The background was described by refining six coefficients of a power series. Two parameters were used to refine the unit cell. One parameter was included to refine the zero point in 2θ. A pseudo-Voigt function[37] was used to describe the peak shapes with the following parameters: three Gaussian half widths (U, V, W), a Lorentzian half-width (L_x), and strain and particle broadening. The structure refinement of $FeWN_2$ included positional coordinates of nitrogen, and isotropic thermal displacement factors for each atom. The refinement converged with $R_{wp} = 8.73\%$, $R_p = 6.65\%$, and $\chi^2 = 3.2$. The data, fit, and residuals are shown in Figure 2, and the structure is shown in Figure 3. The atomic positions are listed in Table 1, and selected bond distances are listed in Table 2.

(b) $MnMoN_2$. The powder X-ray diffraction pattern was indexed to a hexagonal unit cell with $a = 2.92262(8)$ Å, $c = 10.8564(4)$ Å. The indexing and the systematic absences indicated that $MnMoN_2$ is isostructural with β-$MnWN_2$ ($P6_3/mmc$),[31] which was used as the starting model for the refinement. The refinement was carried out in the same fashion as that for $FeWN_2$, with the exception of the specific parameters used for the profile description. To describe the peak profiles of $MnMoN_2$ using the pseudo-Voigt function, the Lorentzian half-width (L_x), the asymmetry, and the grain size broadening were refined. No Gaussian contribution to the peak profile was found. The structure refinement of $MnMoN_2$ utilized the metal atom position found in β-$MnWN_2$ as a starting model.[31] To locate the nitrogen positions, a Fourier difference map, Figure 4, was generated and the main nitrogen atom position was determined. Further Fourier calculations suggest that additional nitrogen positions might exist. However, it is not possible to determine accurately these positions or their fractional occupancies with the available X-ray data. The same problem was encountered by Grins *et al.*[38] in their structure analysis of $MnMoN_2$. To

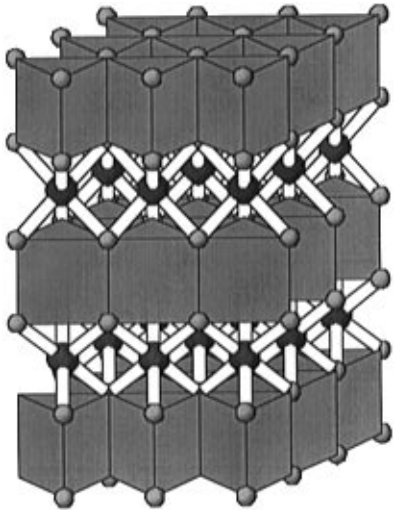

Figure 3. Proposed structure for $FeWN_2$. Trigonal prismatic tungsten are shown as filled polyhedra. The iron and nitrogen positions are indicated by a ball and stick representation. Large gray balls represent iron atoms, and small gray balls represent nitrogen atoms. In $FeWN_2$ the layers are staggered and stacked in the sequence **AcAcBcBcA**, where **A** and **B** represent the close-packed nitrogen atoms and **c** = iron and tungsten.

Table 1. Atomic Positions Based on the X-ray Refinements of $FeWN_2$ ($a = 2.87630(5)$ Å, $c = 10.9320(4)$ Å) and $MnMoN_2$ $a = 2.92262(8)$ Å, $c = 10.8564(4)$ Å)

metal	Wyckoff	x	y	z	$100U_{iso}$, Å^2
		$FeWN_2$ ($P6_3/mmc$)			
Fe	2(a)	0	0	0	2.39(7)
W	2(b)	0	0	$^1/_4$	0.77(3)
N	4(f)	$^1/_3$	$^2/_3$	0.3757(7)	0.3(2)
		$MnMoN_2$ $P6_3/mmc$			
Mn	2(a)	0	0	0	2.09(4)
Mo	2(d)	$^1/_3$	$^2/_3$	$^3/_4$	0.09(2)
N	4(f)	$^1/_3$	$^2/_3$	0.1318(4)	0.1(1)

(37) Thompson, P.; Cox, D. E.; Hastings, J. B. *J. Appl. Crystallogr.* **1987**, *20*, 79.

(38) Grins, J.; Käll, P.-O.; Svensson, G. J. *J. Mater. Chem.* **1995**, *5*, 571.

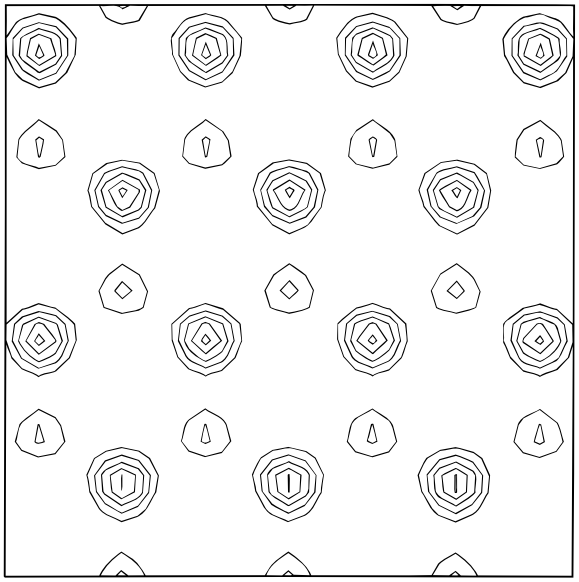

Figure 4. Fourier difference map for $MnMoN_2$ to locate the nitrogen position(s). The nitrogen position is located at $^1/_3$, $^2/_3$, 0.1318(4).

Table 2. Selected Bond Distances (Å)

Fe−Fe	2.87630(5)	W−W	2.87630(5)
Fe−W	2.73301(9)	W−N	2.156(5)
Fe−N	2.145(5)	N−N	2.75(2)
Mn−Mn	2.92262(8)	Mo−Mo	2.92262(8)
Mn−Mo	3.1959(1)	Mo−N	2.120(2)
Mn−N	2.212(3)	N−N	2.566(8)

address this issue further, we will collect neutron data. Table 1 lists the three atomic positions that were used for this refinement, which converged with $R_{wp} = 13.1\%$, $R_p = 10.6\%$, and $\chi^2 = 1.43$. The data, fit, and residuals are shown in Figure 5, and the structure is shown in Figure 6. Selected bond distances are listed in Table 2.

Conductivity Measurements. Temperature-dependent four probe resistance measurements were performed on pressed pellets. The measured conductivities of $FeWN_2$ and $MnMoN_2$ are shown in Figure 7. Both $FeWN_2$ and $MnMoN_2$ exhibit only a very small temperature dependence in their conductivities. The conductivity of $FeWN_2$ is approximately a factor of 10 higher than that of $MnMoN_2$.

Discussion

The Rietveld refinements of these new ternary nitride phases show that they belong to a structurally related family of materials. The idealized structures contain sheets of edge-shared octahedra alternating with layers consisting of edge-shared trigonal prisms. The exact stacking arrangement, however, differs between $FeWN_2$ and $MnMoN_2$. The structure of $FeWN_2$, Figure 3, consists of alternating layers of edge-shared FeN_6 octahedra and WN_6 trigonal prisms, where the octahedra and trigonal prisms are face-shared in the *c*-direction. The arrangement of the nitrogen and metal atoms can be represented by **AcAcBcBcA**, where **A** and **B** represent the close-packed nitrogen atoms and **c** = iron and tungsten. The structure of $MnMoN_2$, Figure 6, similar to that of $FeWN_2$, consists of layers of MnN_6 octahedra and MoN_6 trigonal prisms. However, in $MnMoN_2$ the layers are staggered and stacked in the sequence **AbAcBaBcA**, where **A** and **B** represent the closed packed nitrogen atoms, **c** = manganese, and **a, b** = molybdenum. Other nitrides that exhibit this structural motif with identical or similar stacking sequences include $LiMoN_2$,[5] $(Fe_{0.8}Mo_{0.2})MoN_2$,[36] α- and β-$MnWN_2$,[31] Ta_5N_6, and Nb_5N_6.[31]

The metal−nitrogen bond distances found in $FeWN_2$ and $MnMoN_2$ are similar to those found in structurally related nitrides and in all cases range from about 2.0 to 2.25 Å. The Fe−N bond distance in $FeWN_2$ of 2.145(5) Å is similar to that found for the Fe−N bond in $(Fe_{0.8}Mo_{0.2})MoN_2$,[36] 2.164(4) Å, and likewise the W−N bond of 2.156(5) Å compares well with that found in β-$MnWN_2$, 2.258(2) Å.[39] The Mo−N bond of 2.120(2) Å in $MnMoN_2$, similarly, is comparable to the Mo−N bond lengths of 2.095(4) and 2.091(4) Å found in $LiMoN_2$[5] and of 2.130(3) Å found in $(Fe_{0.8}Mo_{0.2})MoN_2$, and the Mn−N distance of 2.213(3) Å is close to that found in β-$MnWN_2$, 2.118(2) Å. All of the above mentioned nitrides share the same structural motif of MN_2 sheets of trigonal prisms (M = Mo, W) with metal cations occupying the octahedral sites between adjacent sheets.

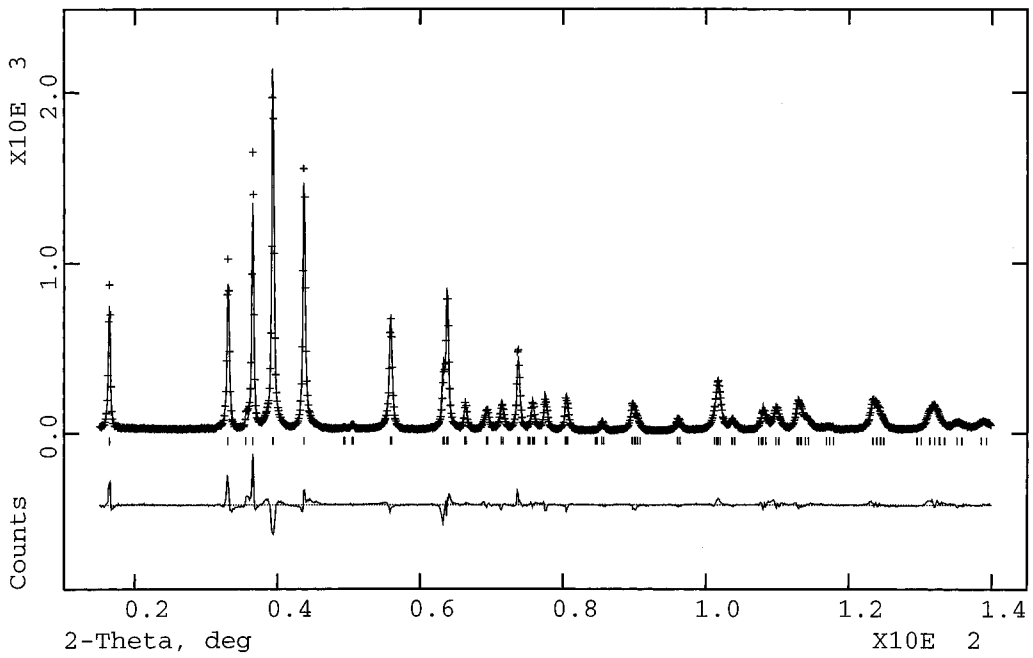

Figure 5. Observed (dotted) and calculated (solid line) X-ray profile for $MnMoN_2$. Tic marks below the diffractogram represent allowed Bragg reflections. The difference line, observed minus calculated, is located at the bottom of the figure.

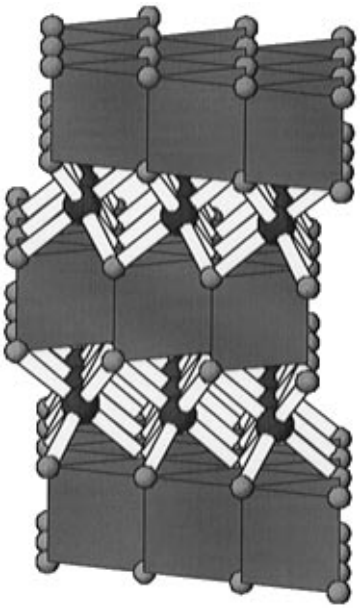

Figure 6. Proposed structure for $MnMoN_2$; Trigonal prismatic molybdenums are shown as filled polyhedra. The manganese and nitrogen positions are indicated by a ball and stick representation. Large gray balls represent manganese atoms, and small gray balls represent nitrogen atoms. In the structure of $MnMoN_2$ the layers are staggered and stacked in the sequence **AbAcBaB**, where **A** and **B** represent the closed-packed nitrogen atoms, **c** = manganese, and **a, b** = molybdenum.

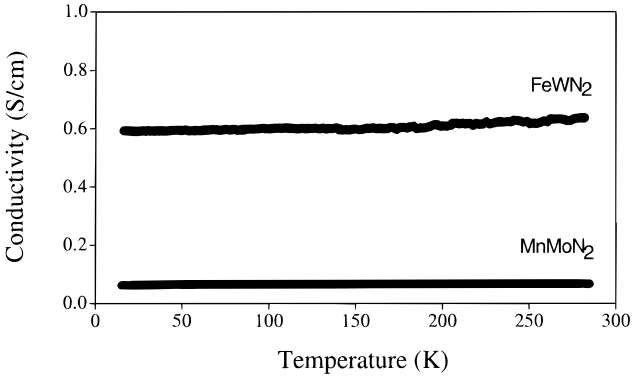

Figure 7. Conductivity data for $FeWN_2$ and $MnMoN_2$ showing temperature-independent conductivity.

In comparison with other ternary transition metal nitrides, this family of nitrides exhibits systematically longer metal−nitrogen bond lengths. For example, in the ternary nitrides Ba_3FeN_3,[40] Li_3FeN_2,[23] Li_4FeN_2,[41] Sr_3MnN_3,[42] Ba_3MnN_3,[42] Na_3MoN_3,[43] Na_3WN_3,[43] Ba_3MoN_4,[44] and Ba_3WN_4,[44] the metal−nitrogen bond distances are Fe−N 1.730(12)−1.957(2) Å, Mn−N 1.741(13)−1.737(12) Å, W−N 1.78(1)−1.93(1) Å, and Mo−N 1.88(1)−1.92(1) Å. The differences in metal−nitrogen bond lengths suggest that the bonding in $FeWN_2$ and $MnMoN_2$ is partially covalent. This is supported by electronic structure calculations reported for $LiMoN_2$,[45] which conclude that the structure consists of strongly covalent MoN_2 sheets with lithium ions between them. Note that the interplanar N−N distances in the trigonal prisms are very short both in $FeWN_2$ (2.75(1) Å) and $MnMoN_2$ (2.566(8) Å) in comparison with the sum of the ionic radii, 2.84−3.08 Å,[46] again consistent with strongly covalent M−N bonds.

Four-probe dc conductivity measurements between 17 and 295 K of both $FeWN_2$ and $MnMoN_2$ show a small temperature dependence (Figure 6) on the order of a few percent. Similar behavior has been observed in the structurally related ternary nitrides $LiMoN_2$,[5] $(Fe_{0.8}Mo_{0.2})MoN_2$,[36] and α,β-$MnWN_2$.[39] While the temperature dependence is consistent with metallic behavior, the conductivity is not exceptionally high for a metal, 0.07−0.6 S/cm. The layered structures of these two nitrides suggest that some anisotropy could be exhibited in the electrical conductivity of the sample. In particular, this should occur for conduction taking place parallel to the covalent trigonal prismatic MN_2 sheets versus that occurring perpendicular to them.[45] Since the measurements were performed on pressed pellets, the data represent an average of all orientations plus a contribution from grain boundary resistance, which may significantly decrease the conductivity. Therefore, our data represent a lower limit of the conductivity of $FeWN_2$ and $MnMoN_2$.

Summary

We have synthesized the new layered ternary transition metal nitrides $FeWN_2$ and $MnMoN_2$ by ammonolysis of ternary transition metal oxides. The structures are proposed on the basis of Rietveld analysis of powder X-ray diffraction data. These compounds are members of a family of layered hexagonal ternary nitrides, consisting of alternating layers of MN_6 (M = Fe, Mn) octahedra and $M'N_6$ (M′ = W, Mo) trigonal prisms.

Acknowledgment is made to the donors of the Petroleum Research Fund, administered by the ACS, for partial support. Additional financial support from DuPont and Hoechst-Celanese is acknowledged. D.S.B. acknowledges 3M and the National Science Foundation for support. Thanks also expressed to Andrew McInnes for collecting the EDX data and Joel Houmes and Steven Trail for insightful comments.

Supporting Information Available: Output for the final Rietveld cycle of the program GSAS for $FeWN_2$ and $MnMoN_2$ (22 pages). Ordering information is given on any current masthead page.

IC9512338

(39) Bem, D. S.; zur Loye, H.-C. Unpublished results, 1995.
(40) Höhn, P.; Kniep, R.; Rabenau, A. *Z. Kristallogr.* **1991**, *196*, 153−158.
(41) Gudat, A.; Kniep, R.; Rabenau, A. *Angew. Chem.* **1991**, *103*, 217−218.
(42) Tennstedt, A.; Röhr, C.; Kniep, R. *Z. Naturforsch., B* **1993**, *48*, 794−796.
(43) Ostermann, D.; Zachwieja, U.; Jacobs, H. *J. Alloys Compd.* **1992**, *190*, 137−140.
(44) Gudat, A.; Höhn, P.; Kniep, R.; Rabenau, A. *Z. Naturforsch., B* **1991**, *46*, 566−572.
(45) Singh, D. J. *Phys. Rev. B* **1992**, *46*, 9332.
(46) Bauer, W. H. *Crystallogr. Rev.* **1987**, *1*, 59.